

# Study of the effect of target shape on smooth pursuit eye movements - Report 1

Adrien Gregorj<sup>1</sup> and Zeynep Yücel<sup>1,2</sup>

<sup>1</sup>Okayama University, Okayama, Japan

<sup>2</sup>Advanced Telecommunication Research Institute International, Kyoto, Japan

February 16, 2024

## 1 Introduction

Humans, as well as other primates, are able to track moving targets by performing what is called smooth pursuit eye movements. Although this can occasionally occur in the absence of a visual stimuli (e.g. when the target is occluded), smooth pursuit movements generally intend to keep a moving object on the fovea (the high acuity area at the centre of the retina). For this purpose, eye's velocity needs to be adapted to match the velocity of the moving target. The cognitive process involved in smooth pursuit is complex and rely on a combination of motosensor feedbacks and predictive mechanisms [2].

It has been shown that, during smooth pursuit, human use information about the current dynamics of the target, such as its position and velocity, to estimate its future position [1]. As a matter of fact, if a target disappears during smooth pursuit, the eye velocity will be maintained at a residual velocity that depends on the last target velocity [3, 1]. Similarly, in [12], authors found that participants were able to predict target motion up to 600 ms after occlusion, when the target was following a circular trajectory at a constant angular velocity.

In [15], authors investigated if choosing specific shape of targets can contribute to reducing eye motions during fixations. They conducted an experiment where participants were asked to fixate on different shapes of targets. They computed spatial dispersion and microsaccade rate during fixations and found that both were reduced when participants were fixating on a target composed of a cross hair and a bull's eye. In our study, we aim to investigate if similar results can be obtained when participants are asked to track a moving target. We hypothesize that, by choosing specific shapes for the moving target, we can ameliorate the smooth pursuit performance of participants.

## 2 Methods

### 2.1 Apparatus

The gaze data of participants (students and staff members of the university) was recorded using a wearable eye-tracking device (Pupil Labs Core device[7]). This device takes the shape of a pair of goggles with three embedded cameras. Two cameras (192x192 px, 120FPS) are used to record videos of the eyes of the wearer while one wide angle lens world camera (1080p, 120FPS, FOV 139°x83°) records its field of view.

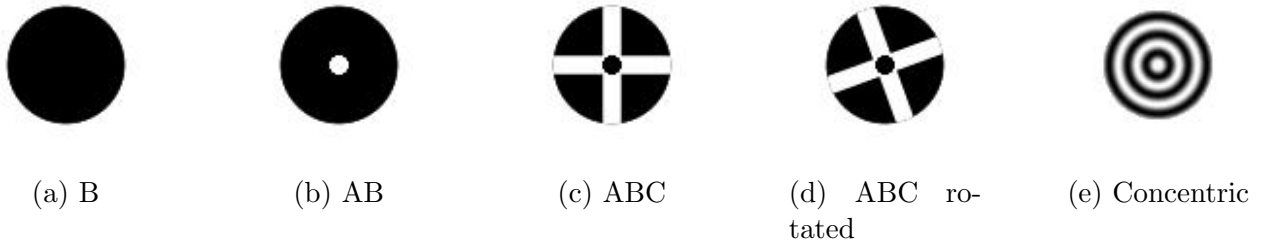


Figure 1: Targets used in the experiment.

The device was connected via USB to a computer that was running the dedicated Pupil Capture software to perform calibration and validation of the gaze data and handle the recording of the experiments (video flux, gaze data, surface tracking).

Participants were seated 60 cm way from the screen on which the stimuli were displayed. Participants' head was constrained using a chin rest to minimize head movements during the experiment.

## 2.2 Stimuli

We used seven different shapes for the moving target, namely:

**B** a plain black circle (see Fig. 1a)

**AB** a circle with a bull's eye (see Fig. 1b)

**ABC** a circle with a bull's eye and a cross hair (see Fig. 1c)

**ABC rotated** a circle with a bull's eye and a cross hair rotated such that one arm of the cross hair was aligned with the direction of motion (see Fig. 1d)

**concentric** a set of concentric circles (see Fig. 1e)

**dilating** a set of concentric circles that dilate, i.e. the target is animated and the concentric circles move away from the center (see Fig. 1e)

**contracting** a set of concentric circles that contract, i.e. the target is animated and the concentric circles move towards the center (see Fig. 1e)

The B, AB, ABC denominations are consistent with the ones used in [15]. The targets are shown in Fig. 1.

The targets have a size of  $1.5^\circ$ .

We follow a procedure similar to the one used in [10]. We use the classic step-ramp paradigm introduced in [14]. The target is first displayed at the center of the screen, with a reduced opacity to signify that the system is waiting for the participant's input. When the participant presses a button, the target becomes fully opaque and the stimulus starts. The target is immobile for a randomized duration (drawn from an exponential distribution with a mean of 3 s, and truncated between 2 and 4 seconds). This serves the purpose of ensuring that the participant is not able to predict the start of the motion. The target is then offset from the center of the screen in a direction opposite to the direction of motion. It then follows a straight trajectory at a constant speed until it is  $10^\circ$  away from the center of the screen. The initial offset is computed such that the target will be at the center of the screen again 200 ms after the start of the

motion. This is done to avoid the initial catch-up saccade that would occur if the target was already directly moved away from the center of the screen.

For each target shape, we use 24 different direction of motion (from 0 to  $\frac{23}{12}\pi$ ) and 5 different speeds (from 16 to 24 °/s, in steps of 2 °/s). This results in a total of 120 different stimuli per target. The stimuli are presented in a randomized order to the participants, in 6 blocks of 20 stimuli. Each block is followed by a break to avoid fatigue. The experiment was repeated on 2 different days, with a minimum of 1 days between the two sessions.

The device was adapted to the face morphology of each participant, in order to obtain a good view of both pupils. Then, each block started with a calibration procedure, using a custom 9 points calibration. These multiple calibration ensure that the tracking performance are not impacted by slippage of the headset, as could be the case if only one calibration was made at the start of the experiment. The calibration procedure was followed by a validation procedure to evaluate the precision and accuracy of the tracking. In cases where the accuracy error was too large ( $> 0.5^\circ$ ) or the precision error was too large ( $> 0.1^\circ$ ), the calibration was restarted. The calibration was restarted a maximum of 3 times, and if the accuracy was still too low, the stimuli were presented anyway.

## 2.3 Data analysis

We removed all data points where the confidence for the pupil detection (provided by the Pupil Labs software) was under a threshold of 0.9 (6.39% percent of all the recorded data).

Pupil Labs' surface tracking plugin reports the gaze position in the normalized coordinate system of the surface denoted  $(\bar{x}, \bar{y})$ , with the origin at the bottom left of the surface (this means that the center of the screen has coordinates  $(0.5, 0.5)$ ).  $(\bar{x}, \bar{y})$  coordinates can be scaled back to actual distance coordinates  $(x, y)$  centered on the screen, by multiplying them by the conversion factors  $f_w = \frac{H_S}{p}$  and  $f_h = \frac{H_S}{p}$  (where  $W_S = 1920$  px,  $H_S = 1080$  px are the pixel dimensions of the screen, and  $p = 55.6$  px/cm is the resolution of the screen) and translating by half the size of the screen.

$$x = f_W \bar{x} - \frac{f_W}{2} = f_W \left( \bar{x} - \frac{1}{2} \right)$$

and

$$y = f_H \bar{y} - f_H/2 = f_H \left( \bar{y} - \frac{1}{2} \right).$$

The participants' face being centered and at a fixed distance  $D = 60$  cm from the screen, we can convert these screen positions to angular coordinates in the spherical reference frame centered on the participant's head by applying the formula  $\phi_x = 2 \arctan\left(\frac{x}{2D}\right)$  and  $\phi_y = 2 \arctan\left(\frac{y}{2D}\right)$ . We note  $\phi = (\phi_x, \phi_y)$  the vector containing the horizontal and vertical angular positions of the gaze.

### 2.3.1 Saccade detection

Saccadic eye motions are characterized by high velocity and acceleration over relatively small period of times. Microsaccades, which are involuntary jerk motions that usually occur during fixations, can be separated from catch-up saccades, which happen during smooth pursuit and aim at reducing the tracking lag with the target of interest. In this work, we use the term saccades to refer to both microsaccades and catch-up saccades.

Saccades can serve as an indicator of the quality of smooth pursuit tracking, as used for instance in [6, 11]. In particular, we measure the saccade rate  $\Sigma$ , which is simply defined as the number of saccades over a given time (usually one second)

Various methods have been proposed to extract saccades from gaze data [5, 13, 8, 4]. In this work, we used the algorithm introduced in [5]. Velocities are first computed by averaging instantaneous velocities across 5 data points, according to the formula  $\dot{\phi}_n = \frac{1}{3} \left( \frac{\phi_{n+2} - \phi_n}{t_{n+2} - t_n} + \frac{\phi_{n+1} - \phi_{n-1}}{t_{n+1} - t_{n-1}} + \frac{\phi_n - \phi_{n-2}}{t_n - t_{n-2}} \right)$ . As our stimuli exhibit significant velocity variations, including acceleration and deceleration of targets, an adaptive threshold approach that adjusts across participants and stimuli rather than relying on absolute thresholds is better suited for our study.

Saccades are then detected in 2D velocity space by using elliptic thresholds based on the median-based standard deviation of the horizontal and vertical velocities. Namely, we compute  $\sigma_{x,y} = \sqrt{\text{med}((\dot{\phi}_{x,y} - \text{med}(\dot{\phi}_{x,y}))^2)}$  where *med* denotes the median of a sample. The thresholds for the velocity components are then computed as  $\lambda_{x,y} = \lambda \sigma_{x,y}$  with  $\lambda = 5$ . Potential saccades are defined as samples for which  $\| \left( \frac{\phi_x}{\lambda_x}, \frac{\phi_y}{\lambda_y} \right) \| \leq 1$ . When plotting the velocity values in 2D space, these corresponds to points that are not inside the ellipse with horizontal axis  $\lambda_x$  and vertical axis  $\lambda_y$ . In addition, are classified as saccades only the events that last longer than 6 ms.

### 2.3.2 Latency and acceleration

We also compute the latency of the pursuit, which is defined as the time it takes for the gaze to start moving after the target starts moving. We do so by following the same method than in [9, 10], which consists of fitting a hinge function to the gaze velocity data and considering the latency to be the time at which the linear part of the hinge function starts, and the acceleration to be the slope of this linear part. To find the optimal fit, we slide a window of 400 ms over the gaze velocity data, and fit the hinge function to the data in this window using a non-linear least square method. We consider the fit that produces the lowest residual error to be the best fit.

### 2.3.3 Steady state

The steady state is the period of time during which the gaze is following the target at a constant velocity. We define the steady state as the period of time starting 300 ms after the start of the motion and lasting 300 ms.

The pursuit gain is then computed as the ratio of the mean gaze velocity during the steady state to the target velocity. The proportion of smooth pursuit is defined as the proportion of motion during the steady state that is classified as smooth pursuit, i.e. without saccades.

## 3 Preliminary results

### 3.1 Fixations

We first analyze the fixations of the participants to verify if we are able to reproduce the results of [15]. We compute the spatial dispersion of the gaze during the fixations, which is defined as the standard deviation of the gaze positions. We also compute the microsaccade rate, which is defined as the number of microsaccades per second. We then compare the results for the different target shapes. The results are shown in Tab. 1.

Considering only the subset of our targets that was studied in [15], i.e. B, AB and ABC, we find that the results are consistent with the ones reported in the paper. Target ABC (circle

Target	Accuracy (°)	Precision (RMS) (°)	Spread (°)	Microsaccade rate (Hz)
B	0.78 ± 0.53	0.13 ± 0.13	0.32 ± 0.29	1.24 ± 1.04
AB	0.71 ± 0.51	0.13 ± 0.15	0.26 ± 0.28	1.01 ± 0.97
ABC	0.67 ± 0.49	0.12 ± 0.10	0.23 ± 0.17	0.72 ± 0.80
ABC rotated	0.71 ± 0.56	0.12 ± 0.09	0.27 ± 0.16	0.69 ± 0.88
contracting	0.65 ± 0.46	<b>0.09 ± 0.08</b>	0.19 ± 0.11	0.86 ± 0.84
dilating	0.59 ± 0.32	0.11 ± 0.11	0.20 ± 0.12	<b>0.66 ± 0.71</b>
concentric	<b>0.54 ± 0.31</b>	0.10 ± 0.10	<b>0.17 ± 0.10</b>	0.68 ± 0.64

Table 1: Spatial dispersion and microsaccade rate for the different target shapes.

with a bull’s eye and a cross hair) exhibits the lowest spatial dispersion and microsaccade rate, while target B (circle) exhibits the worst performance.

We find that overall, the contracting, dilating and concentric targets exhibit the best performance in terms of spatial dispersion and microsaccade rate. Surprisingly, the dilating target exhibits the lowest microsaccade rate, despite the fact that it is an animated target. More data is needed to confirm these results.

### 3.2 Pursuit performance

In Tab. 2, we report the latency, acceleration, pursuit gain and proportion of smooth pursuit for the different target shapes. We find that the ABC rotated target exhibits the best performance in terms of pursuit gain and proportion of smooth pursuit.

## References

- [1] G R Barnes and P T Asselman. “The Mechanism of Prediction in Human Smooth Pursuit Eye Movements.” In: *The Journal of Physiology* 439.1 (July 1, 1991), pp. 439–461. ISSN: 00223751. DOI: [10.1113/jphysiol.1991.sp018675](https://doi.org/10.1113/jphysiol.1991.sp018675). URL: <https://onlinelibrary.wiley.com/doi/10.1113/jphysiol.1991.sp018675> (visited on 03/10/2023).
- [2] G.R. Barnes. “Cognitive Processes Involved in Smooth Pursuit Eye Movements”. In: *Brain and Cognition* 68.3 (Dec. 2008), pp. 309–326. ISSN: 02782626. DOI: [10.1016/j.bandc.2008.08.020](https://doi.org/10.1016/j.bandc.2008.08.020). URL: <https://linkinghub.elsevier.com/retrieve/pii/S0278262608002650> (visited on 02/13/2023).
- [3] W. Becker and A.F. Fuchs. “Prediction in the Oculomotor System: Smooth Pursuit during Transient Disappearance of a Visual Target”. In: *Experimental Brain Research* 57.3 (Feb. 1985). ISSN: 0014-4819, 1432-1106. DOI: [10.1007/BF00237843](https://doi.org/10.1007/BF00237843). URL: <http://link.springer.com/10.1007/BF00237843> (visited on 03/08/2023).
- [4] F. Behrens, M. MacKeben, and W. Schröder-Preikschat. “An Improved Algorithm for Automatic Detection of Saccades in Eye Movement Data and for Calculating Saccade Parameters”. In: *Behavior Research Methods* 42.3 (Aug. 2010), pp. 701–708. ISSN: 1554-351X, 1554-3528. DOI: [10.3758/BRM.42.3.701](https://doi.org/10.3758/BRM.42.3.701). URL: <http://link.springer.com/10.3758/BRM.42.3.701> (visited on 02/13/2023).

Target	Latency (ms)	Acceleration ( $^{\circ}/s^2$ )	Pursuit gain	Proportion of smooth pursuit	Microsaccade amplitude ( $^{\circ}$ )
B	$0.12 \pm 0.03$	$92.62 \pm 59.66$	$0.86 \pm 0.21$	$0.89 \pm 0.08$	$1.84 \pm 1.40$
AB	$0.12 \pm 0.03$	$89.50 \pm 57.00$	$0.84 \pm 0.20$	$0.88 \pm 0.08$	$2.00 \pm 1.37$
ABC	$0.12 \pm 0.03$	$87.46 \pm 45.68$	$0.85 \pm 0.18$	$0.89 \pm 0.08$	$1.82 \pm 1.42$
ABC rotated	$0.12 \pm 0.02$	<b><math>100.04 \pm 52.65</math></b>	<b><math>0.91 \pm 0.19</math></b>	<b><math>0.91 \pm 0.07</math></b>	<b><math>1.55 \pm 1.31</math></b>
contracting	$0.11 \pm 0.02$	$62.75 \pm 57.95$	$0.81 \pm 0.22$	$0.85 \pm 0.08$	$2.36 \pm 1.45$
dilating	$0.12 \pm 0.02$	$53.64 \pm 42.68$	$0.85 \pm 0.31$	$0.85 \pm 0.08$	$2.46 \pm 1.41$
concentric	$0.11 \pm 0.02$	$82.39 \pm 49.85$	$0.79 \pm 0.18$	$0.85 \pm 0.07$	$2.03 \pm 1.10$

Table 2: Measures of pursuit performance for the different target shapes.

- [5] Ralf Engbert and Konstantin Mergenthaler. “Microsaccades are triggered by low retinal image slip”. In: *Proceedings of the National Academy of Sciences* 103.18 (May 2, 2006), pp. 7192–7197. ISSN: 0027-8424, 1091-6490. DOI: [10.1073/pnas.0509557103](https://doi.org/10.1073/pnas.0509557103). URL: <https://pnas.org/doi/full/10.1073/pnas.0509557103> (visited on 02/13/2023).
- [6] Lee Friedman et al. “Relationship between Smooth Pursuit Eye-Tracking and Cognitive Performance in Schizophrenia”. In: *Biological Psychiatry* 37.4 (Feb. 1995), pp. 265–272. ISSN: 00063223. DOI: [10.1016/0006-3223\(94\)00170-8](https://doi.org/10.1016/0006-3223(94)00170-8). URL: <https://linkinghub.elsevier.com/retrieve/pii/0006322394001708> (visited on 03/08/2023).
- [7] Moritz Kassner, William Patera, and Andreas Bulling. “Pupil: An Open Source Platform for Pervasive Eye Tracking and Mobile Gaze-Based Interaction”. In: *Proceedings of the 2014 ACM International Joint Conference on Pervasive and Ubiquitous Computing: Adjunct Publication*. UbiComp ’14 Adjunct. Seattle, Washington: Association for Computing Machinery, 2014, pp. 1151–1160. ISBN: 9781450330473. DOI: [10.1145/2638728.2641695](https://doi.org/10.1145/2638728.2641695). URL: <https://doi.org/10.1145/2638728.2641695>.
- [8] Oleg V. Komogortsev and Alex Karpov. “Automated Classification and Scoring of Smooth Pursuit Eye Movements in the Presence of Fixations and Saccades”. In: *Behavior Research Methods* 45.1 (Mar. 2013), pp. 203–215. ISSN: 1554-3528. DOI: [10.3758/s13428-012-0234-9](https://doi.org/10.3758/s13428-012-0234-9). URL: <http://link.springer.com/10.3758/s13428-012-0234-9> (visited on 02/13/2023).
- [9] R. J. Krauzlis and F. A. Miles. “Release of Fixation for Pursuit and Saccades in Humans: Evidence for Shared Inputs Acting on Different Neural Substrates”. In: *Journal of Neurophysiology* 76.5 (Nov. 1996). DOI: [10.1152/jn.1996.76.5.2822](https://doi.org/10.1152/jn.1996.76.5.2822).
- [10] Dorian B. Liston and Leland S. Stone. “Oculometric Assessment of Dynamic Visual Processing”. In: *Journal of Vision* 14.14 (Dec. 19, 2014), pp. 12–12. ISSN: 1534-7362. DOI: [10.1167/14.14.12](https://doi.org/10.1167/14.14.12).
- [11] Andrew Isaac Meso et al. “Evidence of Inverted Gravity-driven Variation in Predictive Sensorimotor Function”. In: *European Journal of Neuroscience* 52.12 (Dec. 2020), pp. 4803–4823. ISSN: 0953-816X, 1460-9568. DOI: [10.1111/ejn.14926](https://doi.org/10.1111/ejn.14926). URL: <https://onlinelibrary.wiley.com/doi/10.1111/ejn.14926> (visited on 03/08/2023).
- [12] J. J. Orban de Xivry, M. Missal, and P. Lefevre. “A Dynamic Representation of Target Motion Drives Predictive Smooth Pursuit during Target Blanking”. In: *Journal of Vision* 8.15 (Nov. 1, 2008), pp. 6–6. ISSN: 1534-7362. DOI: [10.1167/8.15.6](https://doi.org/10.1167/8.15.6). URL: <http://jov.arvojournals.org/Article.aspx?doi=10.1167/8.15.6> (visited on 03/08/2023).
- [13] Jami Pekkanen and Otto Lappi. “A New and General Approach to Signal Denoising and Eye Movement Classification Based on Segmented Linear Regression”. In: *Scientific Reports* 7.1 (Dec. 18, 2017), p. 17726. ISSN: 2045-2322. DOI: [10.1038/s41598-017-17983-x](https://doi.org/10.1038/s41598-017-17983-x). URL: <https://www.nature.com/articles/s41598-017-17983-x> (visited on 02/13/2023).
- [14] Cyril Rashbass. “The Relationship between Saccadic and Smooth Tracking Eye Movements”. In: *The Journal of Physiology* 159.2 (Dec. 1961), pp. 326–338. PMID: [14490422](https://pubmed.ncbi.nlm.nih.gov/14490422/).
- [15] L. Thaler et al. “What Is the Best Fixation Target? The Effect of Target Shape on Stability of Fixational Eye Movements”. In: *Vision Research* 76 (Jan. 2013), pp. 31–42. ISSN: 00426989. DOI: [10.1016/j.visres.2012.10.012](https://doi.org/10.1016/j.visres.2012.10.012). (Visited on 02/13/2023).